

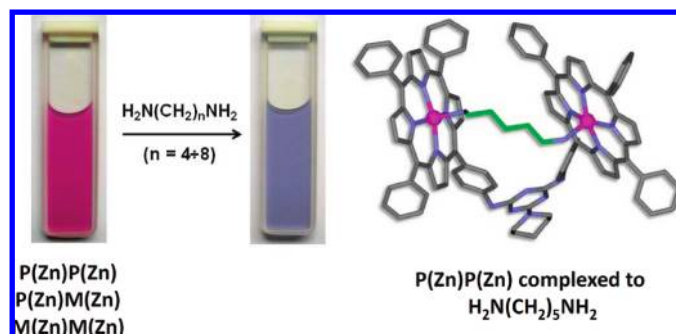
## Melamine-Bridged Bis(porphyrin-Zn<sup>II</sup>) Receptors: Molecular Recognition Properties

Tommaso Carofiglio,\* Elisa Lubian, Ileana Menegazzo, Giacomo Saielli, and Alessandro Varotto

Department of Chemical Sciences and ITM-CNR, University of Padua, Padua, Italy

tommaso.carofiglio@unipd.it

Received August 14, 2009



Dimeric metalloporphyrin hosts with tweezer-like structures have been synthesized by reacting the cyanuric chloride scaffold, CC, with 5-(4-aminophenyl)-10,15,20-triphenylporphyrin, P, and 5-(4-aminophenyl)-10,15,20-trimesitylporphyrin, M, to yield the homoconjugates free bases PP and MM and the heterodiyad PM. Metalation with Zn(II), gives three structurally related ditopic receptors P(Zn)P(Zn), P(Zn)M(Zn), and M(Zn)M(Zn) with differential steric hindrance and conformational rigidity. The solution structure and supramolecular properties of these porphyrin dimers have been investigated as isolated molecules and in the presence of aliphatic  $\alpha,\omega$ -diamines of general formula  $\text{H}_2\text{N}-(\text{CH}_2)_n-\text{NH}_2$  ( $n = 4-8$ ) by spectroscopic and theoretical studies including multidimensional NMR, UV-vis, molecular modeling, and computational NMR methods. Binding constants in the range  $4.2 \times 10^6$  to  $3.4 \times 10^7 \text{ M}^{-1}$  are observed in dichloromethane at 298 K, with a 3 orders of magnitude increase as compared to monodentate  $n\text{BuNH}_2$ , thus indicating the occurrence of a host-guest ditopic interaction. Linear correlation graphs are obtained by plotting the Soret band shift ( $\Delta\nu$ ,  $\text{cm}^{-1}$ ) of the complex as a function of the diamine chain length. Combined NMR evidence and OPLS 2005 Force Field conformational analysis point to a mutual adaptation of both the binding partners in the host-guest complex, whose geometry is mainly dictated by the steric impact of the bulky substituents at the porphyrin periphery.

### Introduction

Metalloporphyrins are frequently used as key motifs for elaborating synthetic molecular receptors<sup>1</sup> by virtue of some unique features: (1) axial ligation fostered by the open coordination site at the metal center in the porphyrin core; (2) specific binding of OH, NH<sub>2</sub> functionalities or other ligands

tailored according to the hard-soft acid-base paradigm; (3) the precise control on the topology and substitution pattern of the receptor, through well-established synthetic methodologies that allow the porphyrin macrocycle to be decorated on demand; and (4) the large aromatic framework of porphyrin ring serving as spectroscopic probe to monitor host-guest complexation by a number of techniques (UV-vis,<sup>2</sup> circular

\*To whom correspondence should be addressed. Phone: 0039498275670. Fax: 0039498275239.

(1) (a) Drain, C. M.; Varotto, A.; Radivojevic, I. *Chem. Rev.* **2009**, *109*, 1630-1658. (b) Beletskaya, I.; Tyurin, V. S.; Tsvadze, Y. A.; Guillard, R.; Stern, C. *Chem. Rev.* **2009**, *109*, 1659-1713. (c) Ogoshi, H.; Kuroda, Y.; Mizutani, T.; Hayashi, T. *Pure Appl. Chem.* **1996**, *68*, 411-415.

(2) (a) Yang, R.; Wang, K.; Long, L.; Xiao, D.; Xiaohai Yang, X.; Tan, W. *Anal. Chem.* **2002**, *74*, 1088-1096. (b) Gulino, A.; Mineo, P.; Bazzano, S.; Daniele Vitalini, D.; Fragalà, I. *Chem. Mater.* **2005**, *17*, 4043-4045. (c) Di Natale, C.; Salimbeni, D.; Paolesse, R.; Macagnano, A.; D'Amico, A. *Sens. Actuators, B* **2000**, *65*, 220-226. (d) Di Natale, C.; Paolesse, R.; D'Amico, A. *Sens. Actuators, B* **2007**, *121*, 238-246.

dichroism,<sup>3</sup> fluorescence,<sup>4</sup> NMR,<sup>5</sup> and resonance Raman spectroscopy<sup>6</sup>).

As a result, a number of single-porphyrin receptors have been developed for the recognition of simple molecules including alcohols,<sup>7</sup> amines,<sup>8</sup> and carbohydrates.<sup>9</sup> In these systems, binding specificity through metal coordination is aided by secondary sterical interactions operated with bulky substituents (*picket-fence*<sup>10</sup> porphyrins), as well as by capping the macrocycle with hydrophobic pockets (*basket-handle*<sup>11</sup> porphyrins). Moreover, decoration of the porphyrin ring with complementary and multiple hydrogen bonding sites implements directionality into the recognition process while improving the selectivity as well. However, these additional secondary interactions play a fundamental role for shape discrimination, but they do not necessarily improve the binding strength of the substrate. In this regard, recognition of multifunctional molecules can take advantage of more than one porphyrin site.<sup>12</sup> A multisite/substrate–receptor mutual interaction guarantees an enhanced binding stability thus allowing the resulting supramolecular assembly to be present as the main entity in solution. For instance, dimeric metalloporphyrin hosts with tweezer-like structures have been designed to effectively complex bifunctional guests through a ditopic interaction. A prominent example among these compounds is the dimeric metalloporphyrin hosts that consist of two achiral zinc-<sup>13</sup> or magnesium-porphyrins<sup>14</sup> linked by a

flexible covalent tether. These constructs have been exploited to assess the absolute stereochemical configuration of chiral amines,<sup>13b,g,h</sup> alcohols,<sup>13g</sup> and carboxylic acids<sup>13i</sup> through the sign of the exciton-coupled circular dichroism in the porphyrin spectral region. Another prosperous field of application for bis-porphyrin hosts deals with the self-assembling of donor–acceptor systems promoted by the  $\pi$ – $\pi$  stacking between a fullerene curved surface and a porphyrin macrocycle.<sup>12a,15</sup> Such fullerene-porphyrin recognition motif has been successfully employed for selective extraction of higher fullerenes,<sup>15c</sup> and to build photovoltaic devices.<sup>15b</sup> Despite these desirable features, the synthesis of porphyrin dimers or oligomers in high yield and purity is often an onerous task imposing multistep procedures and reiterated chromatography purification.

We have recently established a straightforward approach for the modular synthesis of porphyrin dyads<sup>16</sup> that relies on the unique temperature-dependent reactivity of cyanuric chloride, **CC**, toward nucleophiles.<sup>17</sup> Typically, the first chloride reacts rapidly at 0 °C, whereas room temperature or moderate heating (depending on the nucleophile strength) promotes the second substitution. The nucleophilic displacement of the third chloride requires harsher conditions ( $T > 80$  °C for multiple hours). Since quantitative yields are often achieved for these reactions, sequential, one-flask introduction of various substituents into a triazine ring is also feasible.

The benefits of this synthetic methodology are readily envisaged in the design of porphyrin-dyads where the overall stereoelectronic diversity can be generated by a proper synthesis/selection of the isolated components in a homodimer arrangement, by the combination of these within a heterodimeric structure, and/or by differential metalation of the porphyrin units.<sup>16</sup>

Herein, we explore the binding properties of the melamine-bridged bis-porphyrin scaffold as ditopic receptor for bidentate ligands. In particular, the steric constraints of the macrocycle components are expected to affect the conformational stability and binding geometry of the dyad whereby the two porphyrin units are forced into close proximity as a consequence of the recognition event. To this aim, we used two amino-porphyrin building blocks **P** and **M**, respectively carrying phenyl and mesityl *meso*-substituents, to yield the homoconjugates free bases **PP** and **MM** and the heterodyad **PM** (Scheme 1). After metalation with Zn(II), a small library of three structurally related bis-porphyrin receptors is readily obtained, namely **P(Zn)P(Zn)**, **P(Zn)M(Zn)**, and **M(Zn)M(Zn)** derivatives. The steric hindrance at the peripheral positions is supposed to increase steadily from **P(Zn)P(Zn)** to **M(Zn)M(Zn)**, the heterodimer **P(Zn)M(Zn)** being in a midway condition. The binding properties of these receptors have been studied *vis-à-vis* the aliphatic  $\alpha,\omega$ -diamines of general formula  $\text{H}_2\text{N}-(\text{CH}_2)_n-\text{NH}_2$  ( $n = 4-8$ ). Multidimensional NMR spectroscopy techniques combined with molecular

(3) (a) Monsù Scolaro, L.; Andrea Romeo, A.; Pasternack, R. F. *J. Am. Chem. Soc.* **2004**, *126*, 7178–7179. (b) Balaz, M.; Holmes, A. E.; Benedetti, M.; Rodriguez, P. C.; Berova, N.; Nakanishi, K.; Proni, G. *J. Am. Chem. Soc.* **2005**, *127*, 4172–4173.

(4) (a) Zhang, Y.; Yang, R. H.; Liu, F.; Li, K. A. *Anal. Chem.* **2004**, *76*, 7336–7345. (b) Zhou, H.; Baldini, L.; Hong, J.; Wilson, A. J.; Hamilton, A. D. *J. Am. Chem. Soc.* **2006**, *128*, 2421–2425.

(5) (a) Shundo, A.; Labuta, J.; Hill, J. P.; Ishihara, S.; Ariga, K. *J. Am. Chem. Soc.* **2009**, *131*, 9494–9495. (b) Tong, Y.; Hamilton, D. G.; Meillon, J.-C.; Sanders, J. K. M. *Org. Lett.* **1999**, *1*, 1343–1346.

(6) (a) Uchida, T.; Kitagawa, T. *Acc. Chem. Res.* **2005**, *38*, 662–670. (b) Satake, A.; Miyajima, Y.; Kobuke, Y. *Chem. Mater.* **2005**, *17*, 716–724.

(7) (a) Neal, A.; Rakow, N. A.; Suslick, K. S. *Nature* **2000**, *306*, 710–713. (b) Lvova, L.; Di Natale, C.; Paolesse, R.; D'Amico, A. *Sens. Actuators, B* **2006**, *118*, 439–447.

(8) (a) Dunbar, A. D. F.; Richardson, T. H.; McNaughton, A. J.; Hutchinson, J.; Hunter, C. A. *J. Phys. Chem. B* **2006**, *110*, 16646–16651. (b) Bang, J. H.; Lim, S. H.; Park, E.; Suslick, K. S. *Langmuir* **2008**, *24*, 13168–13172. (c) Deviprasad, G. R.; D'Souza, F. *Chem. Commun.* **2000**, 1915–1916.

(9) Mizutani, T.; Kurahashi, T.; Murakami, T.; Noriyoshi Matsumi, N.; Ogoshi, H. *J. Am. Chem. Soc.* **1997**, *119*, 8991–9001.

(10) Collman, J. P. *Inorg. Chem.* **1997**, *36*, 5145–5155.

(11) Rudkevich, D. M.; Verboom, W.; Reinhoudt, D. N. *J. Org. Chem.* **1995**, *60*, 6585–6587.

(12) (a) Hosseini, A.; Taylor, S.; Accorsi, G.; Armaroli, N.; Reed, C. A.; Boyd, P. D. W. *J. Am. Chem. Soc.* **2006**, *128*, 15903–15913. (b) Yagi, S.; Ezoe, M.; Yonekura, I.; Takagishi, T.; Nakazumi, H. *J. Am. Chem. Soc.* **2003**, *125*, 4068–4069. (c) Kuroda, Y.; Kawashima, A.; Hayashi, Y.; Ogoshi, H. *J. Am. Chem. Soc.* **1997**, *119*, 4929–4933. (d) Phillips-McNaughton, K.; Groves, J. T. *Org. Lett.* **2003**, *5*, 1829–1832. (e) Kuramochi, Y.; Satake, A.; Kobuke, Y. *J. Am. Chem. Soc.* **2004**, *126*, 8668–8669.

(13) (a) Yang, Q.; Olmsted, C.; Borhan, B. *Org. Lett.* **2002**, *4*, 3423–3426. (b) Li, X.; Tanasova, M.; Vasileiou, C.; Borhan, B. *J. Am. Chem. Soc.* **2008**, *130*, 1885–1893. (c) Huang, X.; Rickman, B. H.; Borhan, B.; Berova, N.; Nakanishi, K. *J. Am. Chem. Soc.* **1998**, *120*, 6185–6186. (d) Chen, Y.; Petrovic, A. G.; Roje, M.; Pescitelli, G.; Kayser, M. M.; Yang, Y.; Berova, N.; Proni, G. *Chirality* DOI: 10.1002/chir.20718. Published Online: Apr 22, 2009. (e) Petrovic, A. G.; Chen, Y.; Pescitelli, G.; Berova, N.; Proni, G. *Chirality* DOI: 10.1002/chir.20717. Published Online: Apr 22, 2009. (f) Tanasova, M.; Vasileiou, C.; Olumolade, O. O.; Borhan, B. *Chirality* **2009**, *21*, 374–382. (g) Kurtán, T.; Nesnas, N.; Koehn, F. E.; Li, Y.-Q.; Nakanishi, K.; Berova, N. *J. Am. Chem. Soc.* **2001**, *123*, 5974–5982. (h) Huang, X.; Fujioka, N.; Pescitelli, G.; Koehn, F. E.; Williamson, R. T.; Nakanishi, K.; Berova, N. *J. Am. Chem. Soc.* **2002**, *124*, 10320–10335. (i) Yang, Q.; Olmsted, C.; Borhan, B. *Org. Lett.* **2002**, *4*, 3423–3426.

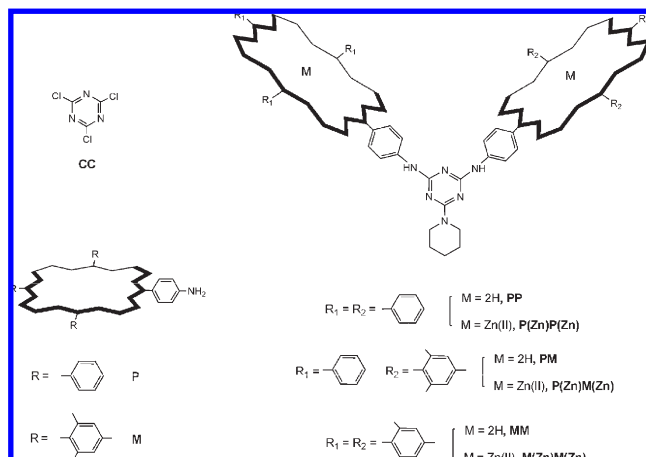
(14) Proni, G.; Pescitelli, G.; Huang, X.; Nakanishi, K.; Berova, N. *J. Am. Chem. Soc.* **2003**, *125*, 12914–12927.

(15) (a) Marois, J.-S.; Cantin, K.; Desmarais, A.; Morin, J.-F. *Org. Lett.* **2008**, *10*, 33–36. (b) Nagata, N.; Kuramochi, Y.; Kobuke, Y. *J. Am. Chem. Soc.* **2009**, *131*, 10–11. (c) Shoji, Y.; Tashiro, K.; Aida, T. *J. Am. Chem. Soc.* **2004**, *126*, 6570–6571. (d) Boyd, P. D. W.; Reed, C. A. *Acc. Chem. Res.* **2005**, *38*, 235–242.

(16) Carofiglio, T.; Varotto, A.; Tonellato, U. *J. Org. Chem.* **2004**, *69*, 8121–8124.

(17) (a) Blotny, G. *Tetrahedron* **2006**, *62*, 9507–9522. (b) Blotny, G. *Tetrahedron Lett.* **2003**, *44*, 1499–1501.

**SCHEME 1. Assembly of Melamine-Bridged Bis-Porphyrin Scaffolds from Selected Building Blocks**



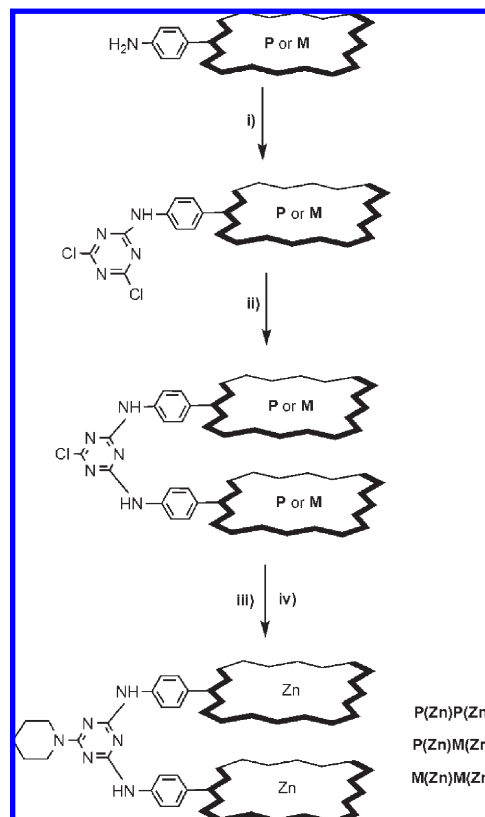
modeling studies have been used to address the solution structure of the supramolecular host–guest complexes. It should be pointed out that among the diamines examined, putrescine (1,4-diaminobutane) and cadaverine (1,5-diaminopentane) are commonly used by trained inspectors and individual consumers for a qualitative evaluation of food freshness, due to their particularly distinctive smells. Accordingly, there is a need for robust sensor devices which accurately, simply, and rapidly, detect the presence of biogenic amines in different food matrices thus enhancing food processing efficiency and giving to the food manufacturers real-time and online information on their products.

## Results and Discussion

**Synthesis and Characterization of the Bis(porphyrin-Zn<sup>II</sup>) Hosts.** The preparation of melamine bridged bis(porphyrin) adducts required the preliminary synthesis of **P** and **M** amino-porphyrin building blocks. In particular, 5-(4-aminophenyl)-10,15,20-triphenylporphyrin,<sup>18</sup> **P**, was obtained in 70% yield by direct mononitration of tetraphenylporphyrin followed by reduction to the corresponding amino-porphyrin with SnCl<sub>2</sub> in concentrated HCl. On the other hand, 5-(4-aminophenyl)-10,15,20-trimesitylporphyrin,<sup>19</sup> **M**, was synthesized in 4.6% yield by using a modification of the Alder–Longo method by reacting pyrrole with a binary mixture of mesitylbenzaldehyde and 4-acetamidobenzaldehyde in the presence of BF<sub>3</sub>·Et<sub>2</sub>O catalyst. The desired monoamidoporphyrin was recovered by preparative column chromatography and hydrolyzed in acidic conditions to produce the corresponding amino-derivative **M**.

Bis(porphyrin) receptors were prepared according to the “one-flask” synthetic protocol outlined in Scheme 2.<sup>16</sup> Briefly, the amino-porphyrin **P** or **M** was reacted with 1 equiv of cyanuric chloride in THF at 0 °C in the presence of diisopropylethylamine (DIPEA). The reaction was stirred at room temperature until TLC analysis indicated the complete disappearance of the starting materials and the formation of the corresponding monoadduct. At this point, a

**SCHEME 2. Synthesis of Melamine-Bridged Porphyrin Dimers<sup>a</sup>**



<sup>a</sup>Reagents and conditions: (i) CC, THF, DIPEA, 0 °C; (ii) **P** or **M**, THF, DIPEA, 80 °C; (iii) piperidine, THF, DIPEA, 80 °C; (iv) Zn(Ac)<sub>2</sub>·2H<sub>2</sub>O, MeOH/CHCl<sub>3</sub>, reflux.

second equivalent of amino-porphyrin derivative (**P** or **M** depending on whether the target molecule was a homodimer, **PP** and **MM**, or a heterodimer, **PM**) was added to the solution and the reaction mixture was stirred at 80 °C for 24 h to afford the corresponding bis(porphyrin) adduct. Finally, the third chloride atom was reacted with piperidine producing a soluble compound (Scheme 2). Noticeably, the third substitution might also afford a convenient route for supporting such porphyrin dimers onto solid materials carrying amino-functionalities, such as Tentagel-amino resin beads, amino-silanized porous glass particles, as well as amino-cellulose. This strategy offers a very convenient route to supported catalysts or chemical sensors.<sup>20</sup>

After standard workup, purification of the crude **PP**, **PM**, and **MM** derivatives was accomplished by preparative column chromatography. Identity and purity of the products were assessed by <sup>1</sup>H NMR spectroscopy, ESI-MS, and HPLC analysis. The isolated yields for **PP**, **PM**, and **MM** dimers were 71%, 88%, and 90% respectively.

Metalation of the porphyrin units was accomplished in quantitative yield by reacting **PP**, **PM**, and **MM** dimers with an excess of Zn(Ac)<sub>2</sub>·2H<sub>2</sub>O in a CHCl<sub>3</sub>/MeOH solvent mixture. The reaction occurs smoothly under reflux conditions as witnessed by (i) the red-shift of the Soret band,

(18) Kruper, W. J.; Chamberlin, T. A.; Kochanny, M.; Lang, K. *J. Org. Chem.* **1989**, *54*, 2753.

(19) Aratani, N.; Osuka, A. *Macromol. Rapid Commun.* **2001**, *22*, 725–740.

(20) Carofiglio, T.; Schiorlin, M.; Tonellato, U. *J. Porph. Phthal.* **2007**, *11*, 749–754.

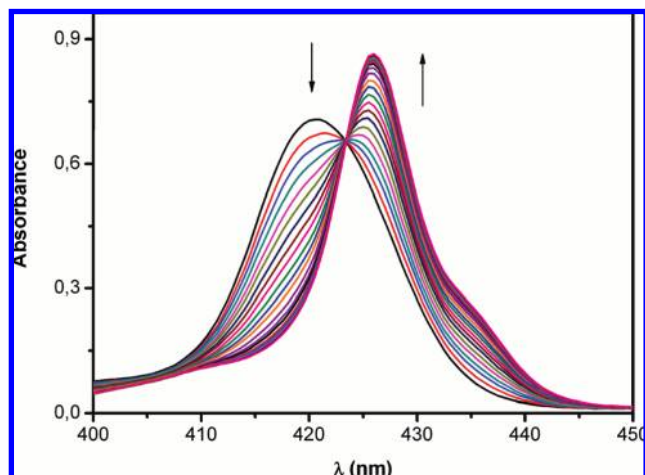


**FIGURE 1.** UV–vis spectra evolution in DCM at 298 K upon titration of **P(Zn)P(Zn)** ( $1.1 \mu\text{M}$ ) with  $\text{H}_2\text{N}(\text{CH}_2)_5\text{NH}_2$  ( $0\text{--}1.7 \mu\text{M}$ ).

**TABLE 1.** Binding Constants ( $\text{M}^{-1}$ ) Determined by Spectrophotometric Titration of **P(Zn)P(Zn)**, **P(Zn)M(Zn)**, and **M(Zn)M(Zn)** with Diamines  $\text{H}_2\text{N}(\text{CH}_2)_n\text{NH}_2$  ( $n = 4\text{--}8$ ) and with Monodentate  $n\text{BuNH}_2$ , in DCM at 298 K

entry	amine	bis( $\text{Zn}^{\text{II}}$ porphyrin), $K$ ( $\text{M}^{-1}$ )		
	$\text{H}_2\text{N}(\text{CH}_2)_n\text{NH}_2$	<b>P(Zn)P(Zn)</b>	<b>P(Zn)M(Zn)</b>	<b>M(Zn)M(Zn)</b>
1	$n = 4$	$4.8 \times 10^6$	n.d. <sup>a</sup>	n.d. <sup>a</sup>
2	$n = 5$	$3.4 \times 10^7$	$8.1 \times 10^6$	$8.5 \times 10^6$
3	$n = 6$	$1.3 \times 10^7$	$2.8 \times 10^7$	$9.0 \times 10^6$
4	$n = 7$	$4.5 \times 10^6$	$7.2 \times 10^6$	$6.9 \times 10^6$
5	$n = 8$	$4.2 \times 10^6$	$5.3 \times 10^6$	$5.2 \times 10^6$
6	$n\text{BuNH}_2$	$3.2 \times 10^4$	$2.7 \times 10^4$	$1.9 \times 10^4$

<sup>a</sup>The binding constant was not determined due to slow binding phenomena (see the discussion in the main text).

(ii) the decrease of the Q-band number from four to two, and (iii) the disappearance of the pyrrolic proton signal in the upfield region of  $^1\text{H}$  NMR spectra.

**Binding Properties of the Bis(porphyrin- $\text{Zn}^{\text{II}}$ ) Hosts.** Zinc-porphyrins are known to coordinate nitrogenous bases to form five-coordinated complexes.<sup>21</sup> Hence, the melamine-bridged bis(porphyrin- $\text{Zn}^{\text{II}}$ ) derivatives are expected to behave as ditopic receptors suitable for binding of diamine ligands. Indeed, a marked color variation from purple to blue was consistently observed upon adding aliphatic  $\alpha,\omega$ -diamines of general formula  $\text{H}_2\text{N}(\text{CH}_2)_n\text{NH}_2$  ( $n = 4\text{--}8$ ) to a dichloromethane (DCM) solution of any of the three bis(porphyrin) receptors. Formation of a receptor-diamine host-guest complex could be studied in DCM, at 298 K, by UV–vis monitoring the characteristic red-shift of the porphyrin Soret band upon diamine complexation. To this purpose, a solution of the bis( $\text{Zn}^{\text{II}}$ -porphyrin) maintained at a constant micromolar concentration was titrated by adding incremental amounts of diamine in DCM. Figure 1 shows a typical spectral change observed for **P(Zn)P(Zn)** upon addition of  $\text{H}_2\text{N}(\text{CH}_2)_5\text{NH}_2$ .

Depletion of the Soret band at 420 nm was accompanied by the formation of a new absorption peak at 426 nm, ascribable to the host-guest complex. The appearance of a sharp isosbestic point at 423 nm is suggestive of a 1:1 binding stoichiometry. The spectral data were analyzed in order to

obtain the value of the binding constant by using the fitting procedure provided by the program HYPERQUAD.<sup>22</sup> This software allows a simultaneous fit of the absorbance values at all the wavelengths as a function of the analytical concentration of the diamine, thus yielding a binding constant calculation with higher precision compared to conventional methods based on a single wavelength monitoring (generally the one corresponding to the most intense absorption peak). The binding constant values for all the hosts with the diamines are collected in Table 1. For comparison purposes, Table 1 also reports the corresponding binding constants for the monodentate  $n\text{BuNH}_2$ .

Scrutiny of data in Table 1 shows that bis(porphyrin- $\text{Zn}^{\text{II}}$ ) receptors display a high affinity toward the aliphatic diamines under examination, with binding constants in the range  $4.2 \times 10^6$  to  $3.4 \times 10^7 \text{ M}^{-1}$ . In contrast, the monodentate benchmark,  $n\text{BuNH}_2$ , binds to the ditopic hosts, with a 3 orders of magnitude smaller constant (entry 6, Table 1). This behavior is likely ascribed to the simultaneous binding of both amino groups of the aliphatic diamine to the two  $\text{Zn}(\text{II})$  recognition sites of the porphyrin dyad, acting as a molecular tweezer. Noteworthy, the association constants found here are 1 or 2 orders of magnitude smaller than those previously reported (for the same series of diamines) with use of a porphyrin tweezer with a flexible pentandiol linker.<sup>23</sup> This is likely due to the interplay of both the rigidity of the melamine bridge and the bulky *meso*-substituents at the porphyrin periphery, which turns out to impart some conformational constraints to the receptors.

A point of interest is the differential binding affinity shown by the three porphyrin dyads with respect to the diamine homologues, which is ascribable both to steric effects on the porphyrinic macrocycles and to the conformational flexibility of the bound diamine. In particular, peak affinities are registered for the short-chain diamines ( $n = 5, 6$ ) binding to the low hindered receptor **P(Zn)P(Zn)**. This latter displays the highest binding constants for the diamine with  $n = 5$  ( $K = 3.4 \times 10^7 \text{ M}^{-1}$ ). On the other hand, the increase of the steric constraints in the **P(Zn)M(Zn)** dimer is responsible for its preferential binding to the diamine with  $n = 6$  ( $K = 2.8 \times 10^7 \text{ M}^{-1}$ ), featuring an elongated alkyl chain and a consequent enhanced conformational flexibility with respect to lower homologues. The **MM** host forms remarkably stable host:guest adducts as well, but without any special preference for any of them. Interestingly, the receptor rigidity seems to affect also the kinetics of the binding process. This is especially apparent in the titration of the **P(Zn)M(Zn)** and **M(Zn)M(Zn)** receptors with the shortest chain diamine ( $n = 4$ , entry 1 in Table 1). Indeed, an immediate and pronounced red-shifting of the Soret band was observed upon addition of the first aliquots of the diamine, followed by a slow blue-shift evolution of the spectrum that required 5–10 min to reach equilibrium. This behavior might result from a fast formation of a 1:1 host:guest complex involving only one of the two amino-groups of the diamine, followed by a slow intramolecular complexation likely hampered by the mesityl substituents at the periphery of the porphyrin macrocycle. For such a reason, these data were considered

(22) Gans, P.; Sabatini, A.; Vacca, A. *Talanta* **1996**, *43*, 1739–1753.

(23) Huang, X.; Borhan, B.; Berova, N.; Nakanishi, K. *J. Indian Chem. Soc.* **1998**, *75*, 725–728.

(21) Weiss, J. J. *Inclusion Phenom. Macro. Chem.* **2001**, *40*, 1–22.

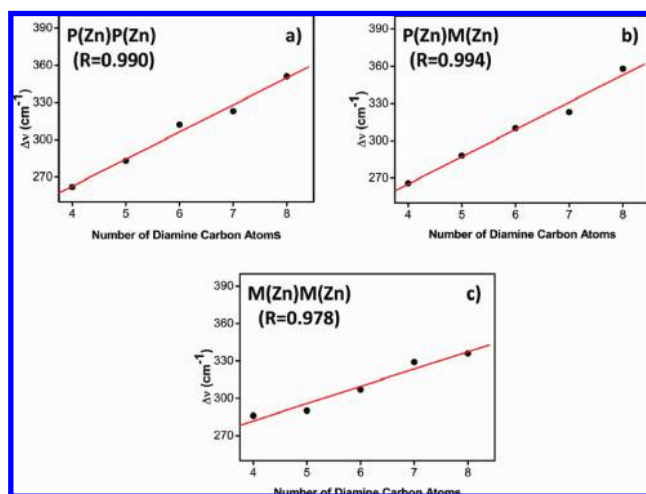


**FIGURE 2.** Variation of the Soret band red-shift ( $\Delta\nu$ ,  $\text{cm}^{-1}$ ) of **P(Zn)P(Zn)**, **P(Zn)M(Zn)**, and **M(Zn)M(Zn)** upon complexation with  $\text{H}_2\text{N}(\text{CH}_2)_n\text{NH}_2$  ( $n = 4-8$ ), as a function of the diamine chain length, in DCM at 298 K. Correlation parameters (slope and correlation coefficient,  $R$ ) are as follows: (a) slope =  $22 \pm 2$ ,  $R = 0.990$ ; (b) slope =  $22 \pm 1$ ,  $R = 0.994$ ; and (c) slope =  $14 \pm 2$ ,  $R = 0.978$ .

inappropriate for an accurate determination of the corresponding binding constants.

As reported in the literature for analogous receptors,<sup>23</sup> the red-shift of the Soret band changes almost linearly with the chain length of the diamine. This fact is the result of two counteracting effects: (i) the amine binding to the metalloporphyrin, which leads to a red shift of the absorption bands, and (ii) the proximity of the two chromophores by effect of the bridging diamine, causing an exciton coupling blue-shift. Figure 2 reports the Soret band shift ( $\Delta\nu$ ,  $\text{cm}^{-1}$ ) for the different porphyrin dimers upon diamine addition. The values have been calculated from the titration data, by evaluating the difference between the wavelength of the Soret band for the free receptor ( $\nu_{\text{free}}$ ) and that at the end of the titration ( $\nu_{\text{complex}}$ ). A table that collects the numerical  $\Delta\nu$  values has been included in the Supporting Information. It is evident from the graphs in Figure 2 that for all three receptors, the  $\Delta\nu$  values change linearly with the number of carbon atoms of the aliphatic diamine.

This approach represents a very simple but useful tool to gather information about the tweezer flexibility. It is clear from these data that the extent of the exciton coupling between the two chromophores decreases as a function of the diamine chain elongation. On the other hand, it is known that the exciton coupling depends both on the distance and the angle between the two interacting chromophores.<sup>24</sup> In this case, due to the rigid nature of the melamine bridge, we expect that the molecular receptor would accommodate the diamine mostly by changing the interplanar angle between the two porphyrin units, as a modification of their distance could be done only to a minor extent. Indeed, according to the correlation graphs in Figure 2, the most hindered receptor **M(Zn)M(Zn)** exhibits a modest response to the diamine structural change (Figure 2c), as it appears from the roughly

halved slope of the linear curve fit. This behavior depends on the mesityl substituent clash, limiting the conformational freedom of the **M(Zn)M(Zn)** tweezer. Since this is a key issue for understanding the molecular recognition properties of this class of receptors, we decided to investigate in more detail their structure by computational modeling.

**Molecular Modeling of the Bis-Porphyrin Dimers and Their Complexes with Diamines.** Inspection of a CPK model of the **P(Zn)P(Zn)** dimer confirmed that the melamine bridge plays a major role in determining the interplanar distance between the two porphyrin units. Indeed, by rotating the porphyrin rings along the C–N bond link of the melamine bridge, it is possible to bring them into a cofacial arrangement at a distance of about 5–6 Å (*syn-syn* conformer in Figure 3). On the other hand, it is also possible to move the two porphyrins far away, at about 19 Å, for the *syn-anti* conformer, or about 21 Å for the *anti-anti* conformer (see Figure 3). In this latter circumstance, however, the piperidine ring would occupy a position between the two porphyrins, thus hampering the distal coordination of an incoming bidentate guest.

A molecular modeling study provided more quantitative information to infer the structure adopted by the bis-(porphyrin) receptors. To this purpose, a conformational search for the **PP** dimer was performed by using a MMFF94 force field as implemented in the SPARTAN'02<sup>25</sup> package and by allowing rotations only about the two triazine-amino and the two amino-phenylporphyrin bonds. It should be pointed out that the conformational analysis was carried out for the free **PP** dimer, rather than for the metalated one, to avoid complications arising from a poor parametrization of Zn(II) in the MMFF94 force field. The energy profile for the **PP** conformers is reported in Figure 4, together with the model structures of three representative conformations. This analysis showed a preferential arrangement with a *syn-syn* structure in which the two porphyrin units are almost parallel to each other. This conformer is almost 5 kcal/mol more stable than a similar *syn-syn* arrangement with a V-shaped disposition of the two porphyrins, and 9 kcal/mol more stable than the *syn-anti* conformer (Figure 4).

Finally, the analysis did not produce any *anti-anti* conformer. The calculated interporphyrin distance in the lower energy *syn-syn* structure was about 6 Å. On the other hand, the CPK models of the aliphatic diamines in extended “zig-zag” all-trans conformation showed that the N–N distance is in the range 6.22–11.22 Å, for  $n = 4$  to 8. Moreover, the Zn–N coordination bond for Zn-porphyrin complexes with amines is typically 2 Å.<sup>26</sup> Therefore, we expect a significant deformation of both the receptor cavity and the diamine ligand in the supramolecular assembly.

A systematic examination of the host–guest structures was undertaken by using molecular modeling methods. The large molecular sizes of the complexes would make these calculations exceedingly computationally demanding if carried out at semiempirical or higher level. However, it has been demonstrated that molecular mechanics calculations with the recently developed OPLS-2005 force field<sup>27</sup> implemented in

(25) Spartan 02; Wavefunction, Inc., www.wavefun.com.

(26) Collins, D. M.; Hoard, J. L. *J. Am. Chem. Soc.* **1970**, *92*, 3761–3771.

(27) Jorgensen, W. L.; Maxwell, D. S.; Tirado-Rives, J. *J. Am. Chem. Soc.* **1996**, *118*, 11225–11236.

(24) Hunter, C. A.; Meah, M. N.; Sanders, J. K. M. *J. Am. Chem. Soc.* **1990**, *112*, 5773–5780.

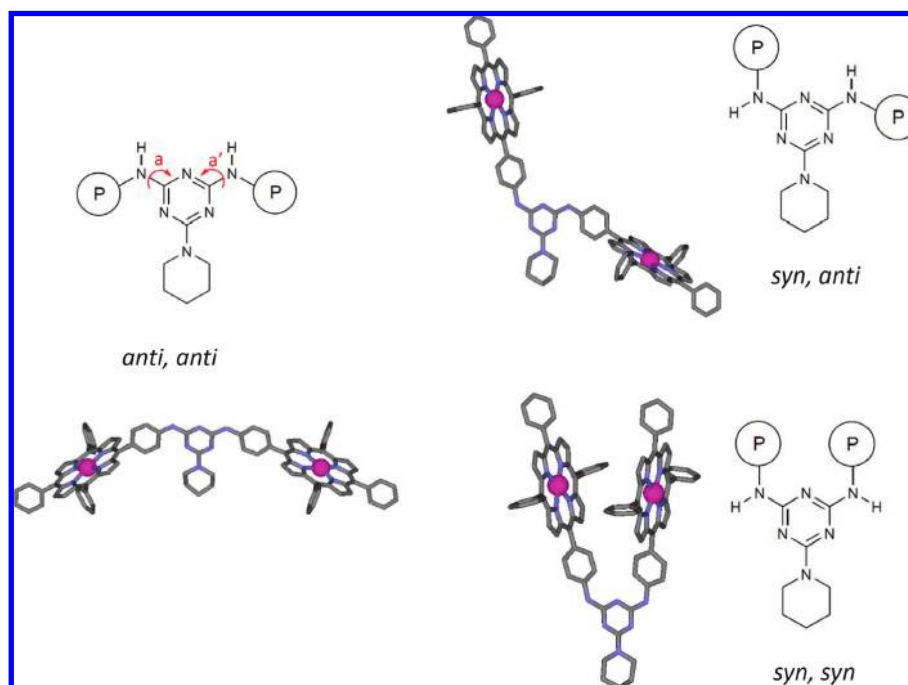


FIGURE 3. CPK models of three limit structures obtained by rotation of triazine–aminoporphyrin bonds (*a* and *a'*).

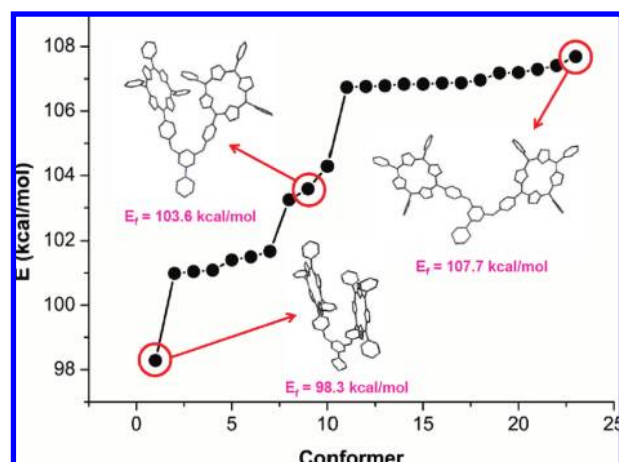


FIGURE 4. Conformational analysis of the **PP** dimer and model structures of three representative conformers.

the MacroModel package<sup>28</sup> can be fairly accurate in describing systems very closely related to our bis(porphyrin-Zn<sup>II</sup>) derivatives. This is especially true since the OPLS-2005 force field incorporates the appropriate parametrization for describing Zn-porphyrin-amine complexes.<sup>13g</sup> Therefore, we subjected to Monte Carlo conformational analysis all the complexes formed between the three host derivatives and the five  $\text{H}_2\text{N}(\text{CH}_2)_n\text{NH}_2$  ( $n = 4-8$ ) guests. Figure 5 depicts the models of the lower energy conformers for the **P(Zn)P(Zn)**, **P(Zn)M(Zn)**, and **M(Zn)M(Zn)** receptors complexed to diamine with  $n = 4$ . This latter case is the most representative to discuss the steric impact of the receptors under examination on the recognition event. For clarity of representation, the

(28) Mohamadi, F.; Richards, N. G. J.; Guida, W. C.; Liskamp, R.; Lipton, M.; Caufield, C.; Chang, G.; Hendrickson, T.; Still, W. C. *J. Comput. Chem.* **1990**, *11*, 440–467.

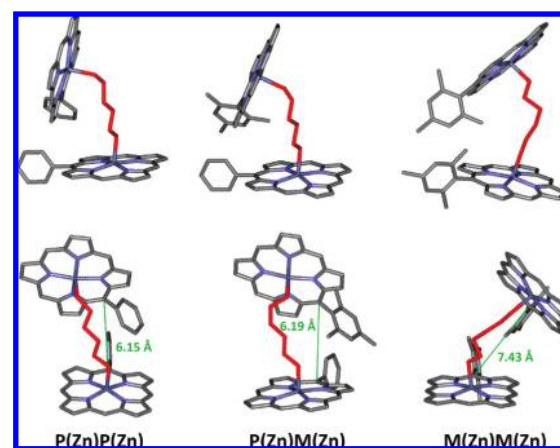


FIGURE 5. Simplified models of the lower energy structures (top = side view, bottom = front view) calculated for the host–guest complexes resulting from the binding of  $\text{H}_2\text{N}(\text{CH}_2)_n\text{NH}_2$  ( $n = 4$ ) to **P(Zn)P(Zn)**, **P(Zn)M(Zn)**, and **M(Zn)M(Zn)** receptors.

model structures do not show the hydrogen atoms, the unnecessary phenyl or mesityl substituents, and the triazine bridge. In the three host–guest complexes, the two porphyrin rings open up in a “V”-shaped conformation where the Zn–Zn distance is about 9 Å. As a consequence of such an arrangement, two of the peripheral phenyl groups come in close contact with each other, and the minimal distance between the two porphyrin planes (arbitrarily measured between the *meso*-carbon atoms carrying these phenyl substituents) turns out to be 6.15, 6.19, and 7.43 Å respectively for **P(Zn)P(Zn)**, **P(Zn)M(Zn)**, and **M(Zn)M(Zn)** (Figure 5).

The longest interplanar distance observed in the case of **M(Zn)M(Zn)** is justified to reduce the steric hindrance between the methyl groups of the mesityl substituents and it is achieved through a twisted distortion of the “V-shaped”

TABLE 2. Results of Monte Carlo Conformational Searches with the OPLS 2005 Force Field

entry	host	guest H <sub>2</sub> N(CH <sub>2</sub> ) <sub>n</sub> NH <sub>2</sub>	$d(\text{Zn}-\text{Zn})_{\text{complex}}$ (Å)	$d(\text{N}-\text{N})_{\text{complex}}$ (Å)	$d(\text{N}-\text{N})_{\text{free}}$ (Å)
1	P(Zn)P(Zn)	4	9.01	6.22	6.21
2		5	9.51	6.59	7.43
3		6	9.55	7.14	8.75
4		7	9.98	7.12	9.98
5		8	10.7	9.10	11.29
6	P(Zn)M(Zn)	4	8.75	5.31	
7		5	9.51	6.42	
8		6	9.96	7.37	
9		7	9.72	7.16	
10		8	10.12	7.59	
11	M(Zn)M(Zn)	4	8.92	5.85	
12		5	9.10	5.45	
13		6	9.66	6.91	
14		7	10.08	7.07	
15		8	11.43	9.17	

porphyrin–porphyrin arrangement (more evident in the front view of Figure 5).

The results of the Monte Carlo conformational searches for all the possible host–guest combinations are reported in Table 2. In particular, the relevant geometrical parameters of the most stable structures include the Zn–Zn distance,  $d(\text{Zn}-\text{Zn})$ , and the N–N distance of the diamine substrate in the host–guest complex,  $d(\text{N}-\text{N})_{\text{complex}}$ . For comparison purposes, also the N–N distance of the free diamine,  $d(\text{N}-\text{N})_{\text{free}}$ , has been calculated for the extended all-trans conformers. Data in Table 2 show that, for all receptors, the  $d(\text{Zn}-\text{Zn})$  increases upon binding of diamines with incremental chain length. This behavior is consistent with the experimental trend registered for the Soret band red-shift ( $\Delta\nu$ ) described in the previous paragraph, thus validating the computational studies. As far as the diamines are concerned, we note that in general  $d(\text{N}-\text{N})_{\text{complex}} < d(\text{N}-\text{N})_{\text{free}}$ . The only exception is observed in the case of the P(Zn)P(Zn)-H<sub>2</sub>N(CH<sub>2</sub>)<sub>4</sub>NH<sub>2</sub> complex (entry 1) where  $d(\text{N}-\text{N})_{\text{complex}} \approx d(\text{N}-\text{N})_{\text{free}}$ . Hence, the formation of the host–guest adduct is not only related to the differences between the steric features of the receptors, but it is also affected by the conformational flexibility of the bound diamines. As a matter of fact, the formation of the host–guest adduct requires an adaption of both the binding partners. In particular, the host increases the  $d(\text{Zn}-\text{Zn})$  by assuming a V-shaped configuration and/or by twisting the two porphyrin rings in order to minimize the steric interactions between the bulky substituents. Conversely, the diamine modifies its more stable extended conformation by assuming a more compact shape with some *s-cis* carbon–carbon bonds.

**Solution Studies by NMR Spectroscopy.** The solution structure of the supramolecular complex has been further addressed by NMR spectroscopy. We focused on the solution behavior of the free P(Zn)P(Zn) receptor and on the formation of the host–guest complex with H<sub>2</sub>N(CH<sub>2</sub>)<sub>5</sub>NH<sub>2</sub>. This latter is characterized by the highest binding constant among all the supramolecular complexes under examination.

The <sup>1</sup>H NMR spectrum of free P(Zn)P(Zn) dimer freshly prepared in CHCl<sub>3</sub> at 298 K is shown in Figure 6a, together with the resonance assignments obtained by two-dimensional homonuclear correlation spectroscopy techniques (DQF-COSY). The spectrum shows three main sets of signals: (i) the porphyrin β-pyrrolic-protons, around 9 ppm, (ii) the porphyrin phenyl protons, in the 8.5–7 ppm

region, and (iii) the piperidine methylenic protons, at 3.94 and 1.75 ppm. The <sup>1</sup>H NMR spectrum of free diamine in CHCl<sub>3</sub> at 298 K is also reported in Figure 3b. The resonance assignments have been carried out by <sup>1</sup>H–<sup>1</sup>H COSY and DQF-COSY.

Noteworthy, at millimolar concentration, the P(Zn)P(Zn) dimer undergoes aggregation phenomena, which result in the progressive broadening of the NMR signal and ultimately yield a massive precipitation of a porphyrin-based material. On the other hand, addition of the diamine guest induces the reversible dissolution of this precipitate, by effect of supramolecular complexation. This behavior is also reflected in the NMR titration experiments outlined in Figure 7.

The evolution of the NMR spectrum during the titration experiments can be conveniently discussed by analyzing the two separate regions pertaining to the aromatic resonances of the receptor from 9.5 to 7.0 ppm, and to the bound diamine signals found between –1.0 and –6.0 ppm (Figure 7).

Upon incremental addition of the diamine, up to 1 equiv, the aromatic host region shows two distinct sets of chemical shifts, corresponding to the protons of free host and to those of the host–guest assembly (Figure 7a–d). For the latter complex, the new resonances build up at significant upfield chemical shift. Precisely, the amount of shifting was about 0.25 ppm for the pyrrolic protons, whereas the aromatic protons shifted upfield to a smaller extent (0.12–0.16 ppm) (Figure 7). This effect is associated with the proximity of the two porphyrin π-systems, upon diamine binding, causing the signals to experience a large ring-current induced shift.<sup>29</sup> A further remark is that broadening of all the aromatic signals is observed as well. In this respect, speciation of the receptor may be complicated by aggregation phenomena, occurring in the time course of the titration experiments. A key observation is that upon reaching the 1:1 host–guest ratio, the resulting NMR spectrum contains just the aromatic signals ascribable to the supramolecular complex, where the *ortho* and *meta* protons of the *meso*-phenyl substituents become nonequivalent, and give rise to sharp multiplets (Figure 7e). Similar splitting is often observed in porphyrin systems with nonequivalent faces.<sup>30</sup>

(29) Ballester, P.; Costa, A.; Deyà, P. M.; Frontera, A.; Gomila, R. M.; Oliva, A. I.; Sanders, J. K. M.; Hunter, C. A. *J. Org. Chem.* **2005**, *70*, 6616–6622.

(30) Ballester, P.; Costa, A.; Castilla, A. M.; Deyà, P. M.; Frontera, A.; Gomila, R. M.; Hunter, C. A. *Chem.—Eur. J.* **2005**, *11*, 2196–2206.

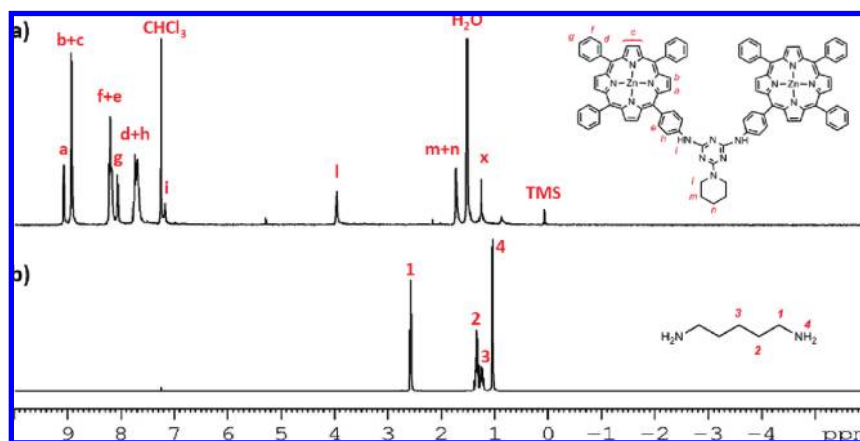


FIGURE 6.  $^1\text{H}$  NMR (400 MHz,  $\text{CDCl}_3$ ) of (a)  $\text{P}(\text{Zn})\text{P}(\text{Zn})$  and (b)  $\text{H}_2\text{N}(\text{CH}_2)_5\text{NH}_2$  together with the resonance assignments according to H–H COSY and DQF-COSY (X denotes an impurity).

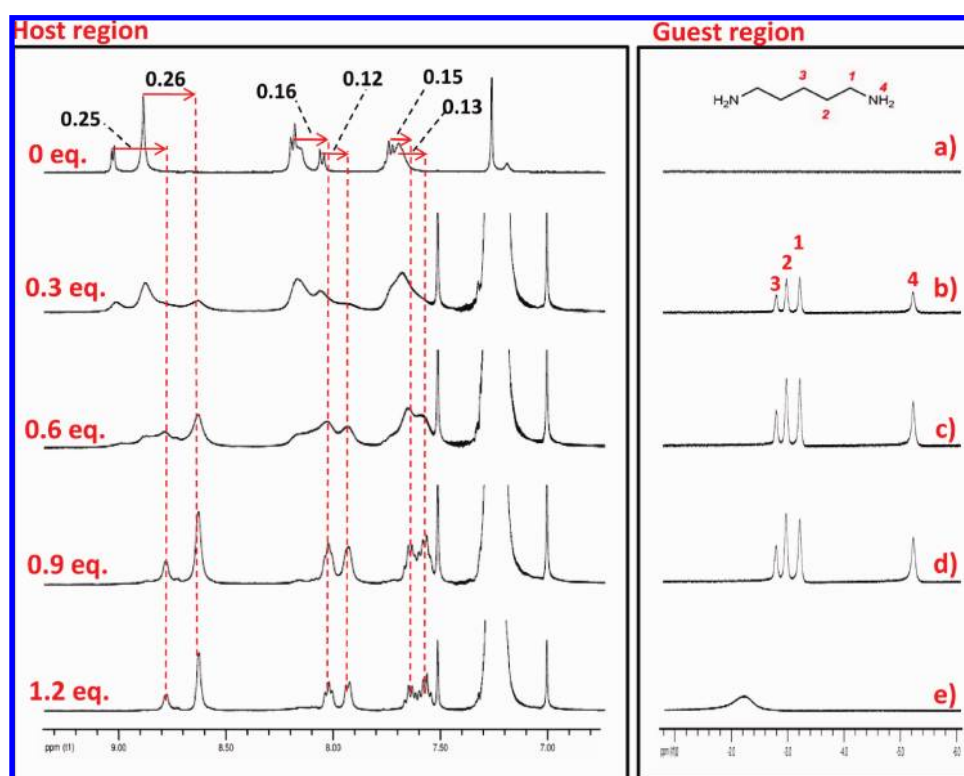


FIGURE 7. Signal changes in the host and guest region during the  $^1\text{H}$  NMR (400 MHz,  $\text{CDCl}_3$ ) titration of  $\text{P}(\text{Zn})\text{P}(\text{Zn})$  (0.1 mM) with  $\text{H}_2\text{N}(\text{CH}_2)_5\text{NH}_2$ . Spectra a, b, c, d, and e respectively represent the  $^1\text{H}$  NMR spectra acquired after adding 0.0, 0.3, 0.6, 0.9, and 1.2 equiv of diamine.

The signals of the diamine protons, in turn, exhibit significant upfield shifts by effect of complexation, due to ring-current anisotropy from porphyrin  $\pi$ -planes.<sup>31</sup> Indeed, with substoichiometric diamine, the guest signals are found between  $-2$  and  $-5$  ppm chemical shift (Figure 7a–d). This evidence is consistent with the bidentate amine being bound within the  $\text{P}(\text{Zn})\text{P}(\text{Zn})$  concave, via ditopic interaction, and exposed to the ring-current effects of porphyrin macrocycles. The resonances of the diamine, while complexed within the host, could be assigned by DQF-COSY and TOCSY experiment as reported in Figure 7.

On the basis of this assignments, we could quantify the upfield shift of the methylene groups (Figure 8). The order of shift found experimentally is  $\text{H}^1 > \text{H}^2 > \text{H}^3$ . Interestingly, above 1 equiv of diamine, the guest signals coalesce due to a fast exchange equilibrium and cannot be observed separately (Figure 7e).

We decided to investigate further, by computational methods, the strong high-field shift induced by the extended  $\pi$  system of the porphyrin rings to the resonances of the diamines.<sup>32</sup> Shielding calculations require high level DFT methods<sup>33</sup> and,

(31) Packer, M. J.; Zonta, C.; Hunter, C. A. *J. Magn. Reson.* **2003**, *162*, 102–112.

(32) Gomila, R. M.; Garau, C.; Frontera, A.; Quinonero, D.; Ballester, P.; Costa, A.; Deyà, P. M. *Tetrahedron Lett.* **2004**, *45*, 9387–9390.

(33) Bagno, A.; Saielli, G. *Theor. Chem. Acc.* **2007**, *117*, 603–619.

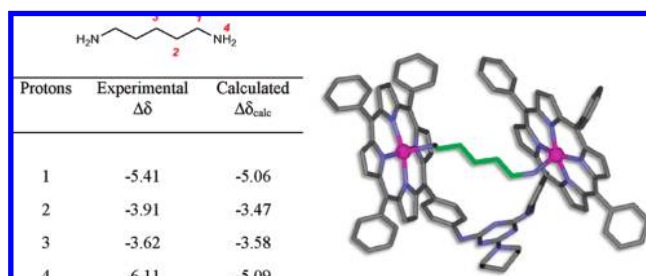


**FIGURE 8.** Energy-minimized conformation obtained for the **P(Zn)P(Zn)**– $\text{H}_2\text{N}(\text{CH}_2)_5\text{NH}_2$  host–guest complex, and experimental versus calculated  $\Delta\delta$  values evaluated for the free and bonded diamine ligand.

in turn, considering the size of the complexes, a high computational effort, especially if relativistic effects are considered. Thus, we have first tested the effect of relativity on the proton chemical shifts by running zeroth-order regular approximation (ZORA)<sup>34</sup> calculations at the Scalar and Spin–Orbit level (BLYP/TZ2P).<sup>35</sup> To this end, we have first considered a simplified model system made by a single Zn-porphyrin having an ethylamine bound to the Zn ion. Comparison of nonrelativistic results with those obtained at the Scalar and Spin–Orbit level reveals that relativistic effects can be safely ignored. Indeed, relativistic proton chemical shifts, even for the  $\text{NH}_2$  protons, the closest to the heavy atoms, differ only by less than 0.1 ppm from the nonrelativistic results. We run shielding calculations for the most stable conformer resulting from the conformational analysis carried out with MacroModel (Figure 8). Relative chemical shifts,  $\Delta\delta$ , observed for the free and complexed diamine are then evaluated. Comparisons of calculated and experimental  $\Delta\delta$  values stand in good agreement (Figure 8). Moreover the strong deshielding of the signals and the general trend as a function of the distance is correctly reproduced, although a somewhat larger error is found for the  $\text{NH}_2$  protons.

## Conclusions

A general approach to the construction of a new class of molecular tweezers has been demonstrated by nucleophilic substitution of the triazine scaffold with tailored aminoporphyrin subunits. Stereoelectronic diversity of the ditopic receptor is readily accessed by the systematic variation of the porphyrin substituents, and homo- or heterocombination of the two appended porphyrin moieties. The Zn(II) derivatives under examination provide an enhanced binding interaction with  $\alpha,\omega$ -aliphatic diamines, resulting in supramolecular complexes with more than 3-order of magnitude higher stability constants as compared to the monodentate reference amine. The influence of the porphyrin substituents on the conformational mobility of the resulting dimeric receptor and on their recognition capabilities has been demonstrated by structure–reactivity correlation, NMR solution speciation, and computational studies. Utility of the title tweezers for the molecular recognition of diamines with rigid spacers and for the determination of the

absolute stereochemical determination of chiral guests as well as their potential for the construction of multicomponent sensing arrays for biogenic amine detection are currently under study.

## Experimental Section

**Bis(phenyl-porphyrin) Homodimer, PP.** The synthesis and characterization of this compound were already reported.<sup>16</sup> We add here the ESI-MS analysis ( $\text{CH}_3\text{CN} + 1\% \text{HCOOH}$  as eluent): 1420.7 (calcd for  $\text{C}_{96}\text{H}_{71}\text{N}_{14}^+ - [\text{MH}]^+$  1420.68), 710.8 (calcd for  $[\text{MH}_2]^{2+}$  710.84), 474.1 (calcd for  $[\text{MH}_3]^{3+}$  474.32).

**Bis(phenylporphyrin-Zn<sup>II</sup>) Homodimer, P(Zn)P(Zn).** The synthesis and characterization of this compound were already reported.<sup>16</sup> We add here the ESI-MS analysis ( $\text{CH}_3\text{CN} + 1\% \text{HCOOH}$  as eluent): 1547.4 (calcd for  $\text{C}_{96}\text{H}_{71}\text{N}_{14}\text{Zn}_2^+ - [\text{MH}]^+$  1547.47), 774.4 (calcd for  $[\text{MH}_2]^{2+}$  774.2), 516.1 (calcd for  $[\text{MH}_3]^{3+}$  516.5).

**(Phenyl-porphyrin)(mesityl-porphyrin) Heterodimer, PM.** To a solution of porphyrin **P** (10 mg, 13  $\mu\text{mol}$ ) in THF (1.0 mL) cooled at 0 °C were added a THF solution of cyanuric chloride (2.4 mg, 13  $\mu\text{mol}$ ) and DIPEA (2 mg, 16  $\mu\text{mol}$ ). After being stirred for 10 min at 0 °C, the solution was left to reach room temperature. TLC analysis (silica gel, petroleum ether/ethyl acetate 3:1 v/v) showed the disappearance of porphyrin **P** ( $R_f$  0.33) and the formation of a new TLC spot at  $R_f$  0.7 corresponding to the monoadduct derivative between **P** and cyanuric chloride. One equivalent of porphyrin **M** (8.3 mg, 13  $\mu\text{mol}$ ) was then added together with 1.2 equiv of DIPEA and the reaction was stirred at 80 °C for 24 h, then an excess of piperidine (3.3 mg, 39  $\mu\text{mol}$ ) was added together with 1.2 equiv of DIPEA (6.2 mg, 48  $\mu\text{mol}$ ) and the mixture was stirred at 80 °C for a further 3 h. The solvent was evaporated and the purple solid was purified by flash silica gel chromatography (silica gel, petroleum ether/ethyl acetate 3:1 v/v) to afford 18 mg of **PM** derivative (88% yield). <sup>1</sup>H NMR ( $\text{CDCl}_3$ , 250 MHz,  $\delta$ ) 8.84 (m, 4H,  $\beta$ -pyrrole), 8.68–8.61 (m, 12H,  $\beta$ -pyrrole), 8.22–8.06 (m, 21H, phenyl aromatic protons), 7.77–7.67 (m, 8H, phenyl amino), 4.00 (br s, 4H, piperidine), 2.62 (s, 9H, mesityl), 1.84 (br s, 18H, mesityl), 1.74 (s, 6H, piperidine), –2.54 (s, 2H, pyrrole mesitylporphyrin), –2.75 (s, 2H, pyrrole phenylporphyrin). ESI-MS ( $\text{CH}_3\text{CN} + 1\% \text{HCOOH}$  as eluent): 1546.8 (calcd for  $\text{C}_{105}\text{H}_{89}\text{N}_{14}^+ - [\text{MH}]^+$  1546.92), 773.9 (calcd for  $[\text{MH}_2]^{2+}$  773.96), 516.1 (calcd for  $[\text{MH}_3]^{3+}$  516.32), 387.4 (calcd. for  $[\text{MH}_4]^{4+}$  387.49). UV–vis ( $\text{CH}_2\text{Cl}_2$ , nm) 420, 516, 552, 593, 647. Anal. Calcd for  $\text{C}_{105}\text{H}_{88}\text{N}_{14}$ : C, 81.58; H, 5.74; N, 12.68. Found: C, 81.33; H, 5.90; N 12.70.

**(Phenyl-porphyrin-Zn<sup>II</sup>)(mesityl-porphyrin-Zn<sup>II</sup>) Heterodimer, P(Zn)M(Zn).** To a solution of **PM** (10 mg, 7  $\mu\text{mol}$ ) in  $\text{CHCl}_3$  (5 mL) was added a saturated solution of zinc acetate dihydrate (in  $\text{CH}_3\text{OH}$  0.5 mL) then the mixture was refluxed for 1 h. After removing the solvent, the residue was dissolved with  $\text{CH}_2\text{Cl}_2$  and washed with water in order to remove the excess of zinc salt. The organic phase was dried over  $\text{Na}_2\text{SO}_4$  then filtered and the solvent was evaporated under reduced pressure to give a purple solid that was purified by short column chromatography on silica gel (eluent:  $\text{CHCl}_3$ ). Yield: 97%. <sup>1</sup>H NMR ( $\text{CDCl}_3$ , 250 MHz):  $\delta$  8.84 (m, 4H,  $\beta$ -pyrrole), 8.68–8.61 (m, 12H,  $\beta$ -pyrrole), 8.22–8.06 (m, 21H, phenyl aromatic protons), 7.77–7.67 (m, 8H, phenyl amino), 4.00 (br s, 4H, ortho piperidine), 2.62 (s, 9H, *p*-methylphenyl), 1.84 (br s, 18H, *o*-methylphenyl), 1.74 (s, 6H, *m*/*p*-piperidine). UV–vis ( $\text{CH}_2\text{Cl}_2$ , nm): 423 ( $\epsilon$  1 168 000  $\text{M}^{-1} \text{cm}^{-1}$ ), 551, 592. ESI-MS ( $\text{CH}_3\text{CN} + 1\% \text{HCOOH}$  as eluent): in the acidic conditions needed for the analysis demetalation of the compound. Anal. Calcd for  $\text{C}_{105}\text{H}_{84}\text{N}_{14}\text{Zn}_2$ : C, 75.39; H, 5.06; N, 11.72. Found: C, 75.00; H, 4.90; N 11.95.

**Bis(mesityl-porphyrin) homodimer, MM.** To a solution of porphyrin **M** (10 mg, 13  $\mu\text{mol}$ ) in THF (1.0 mL) cooled at 0 °C were added a THF solution of cyanuric chloride (2.4 mg,

(34) de Velde, G.; Bikelhaupt, F. M.; Baerends, E. J.; Fonseca Guerra, C.; van Gisbergen, S. J. A.; Snijders, J. G.; Ziegler, T. J. *Comput. Chem.* **2001**, *22*, 931–967.

(35) (a) Becke, A. D. *Phys. Rev. A* **1998**, *38*, 3098–3100. (b) Lee, C.; Yang, W.; Parr, G. *Phys. Rev. B* **1988**, *37*, 785–789. (c) Michlich, B.; Savin, A.; Stoll, H.; Preuss, H. *Chem. Phys. Lett.* **1989**, *157*, 200–206.

13  $\mu\text{mol}$ ) and DIPEA (2 mg, 16  $\mu\text{mol}$ ). After being stirred for 10 min at 0 °C, the solution was left to reach room temperature. The reaction was complete, as resulting from TLC analysis (silica gel, petroleum ether/ethyl acetate 5:1 v/v) showing the disappearance of porphyrin **M** ( $R_f$  0.38). A second equivalent of porphyrin **M** (10 mg, 13  $\mu\text{mol}$ ) was then added together with 1.2 equiv of DIPEA and the reaction was stirred at 80 °C for 24 h then an excess of piperidine (3.4 mg, 39  $\mu\text{mol}$ ) was added together with 1.2 equiv of DIPEA and the mixture was stirred at 80 °C for 3 h. After removal of the solvent, the residue was purified by flash silica gel chromatography (eluent: petroleum ether/ethyl acetate 5:1 v/v) affording 20 mg of **MM** derivative. Yield: 90%.  $^1\text{H}$  NMR ( $\text{CDCl}_3$ , 250 MHz):  $\delta$  8.88 (m, 4H,  $\beta$ -pyrrole), 8.69–8.62 (m, 12H,  $\beta$ -pyrrole), 8.21–8.04 (m, 20H, phenyl aromatic protons), 7.05 (br s, 2H, NH), 3.99 (br s, 4H, piperidine), 2.61 (s, 18H, mesityl), 1.84 (br s, 36H, mesityl), 1.74 (s, 6H, piperidine), –2.56 (s, 4H, pyrrole NH). ESI-MS ( $\text{CH}_3\text{CN} + 1\%$  HCOOH as eluent): 1672.9 (calcd for  $\text{C}_{114}\text{H}_{107}\text{N}_{14}^+ - [\text{MH}]^+$  1673.16), 837.0 (calcd for  $[\text{MH}]^{2+}$  837.08), 558.3 (calcd for  $[\text{MH}]^{3+}$  558.39), 419.0 (calcd for  $[\text{MH}]^{4+}$  419.05). UV–vis ( $\text{CH}_2\text{Cl}_2$ , nm): 420, 516, 550, 593, 648. Anal. Calcd for  $\text{C}_{114}\text{H}_{106}\text{N}_{14}$ : C, 81.88; H, 6.39; N, 11.73. Found: C, 82.10; H, 6.52; N 12.03.

**Bis(mesityl-porphyrin-Zn<sup>II</sup>) Homodimer, M(Zn)M(Zn).** This derivative was prepared from **MM** following the same procedure described for compound **P(Zn)P(Zn)**. Yield: 97%.  $^1\text{H}$  NMR ( $\text{CDCl}_3$ , 250 MHz):  $\delta$  8.98 (m, 4H,  $\beta$ -pyrrole), 8.78–8.71 (m, 12H,  $\beta$ -pyrrole), 8.23–8.06 (m, 20H, phenyl aromatic protons), 7.07 (br s, 2H, NH), 4.00 (br s, 4H, piperidine), 2.63 (s, 18H, mesityl), 1.85 (br s, 36H, mesityl), 1.74 (s, 6H, piperidine). ESI-MS ( $\text{CH}_3\text{CN} + 1\%$  HCOOH as eluent): 1799.9 (calcd for

$\text{C}_{114}\text{H}_{103}\text{N}_{14}\text{Zn}_2^+ - [\text{MH}]^+$  1799.95). UV–vis ( $\text{CH}_2\text{Cl}_2$ , nm) 423 ( $\epsilon$  1 121 000  $\text{M}^{-1} \text{cm}^{-1}$ ), 550, 593. Anal. Calcd for  $\text{C}_{114}\text{H}_{102}\text{N}_{14}\text{Zn}_2$ : C, 76.11; H, 5.72; N, 10.90. Found: C, 76.60; H, 5.46; N, 10.75.

**Acknowledgment.** Financial support for this project came from the University of Padua (Progetti di Ricerca di Ateneo-CPDA088228/08 and Progetti Strategici 2008-HELIOS). We thank Dr. Arianna Bassan and Dr. Elena Fioravanzo for helpful discussions about the use of MacroModel software. NMR shielding calculations were run on the Linux cluster of the Laboratorio Interdipartimentale di Chimica Computazionale of the Department of Chemical Sciences, University of Padova.

**Supporting Information Available:** Description of the General Experimental Methods,  $^1\text{H}$  NMR spectra, ESI-MS and HPLC analyses for free and Zn(II) receptors (Figures S1–S14),  $^1\text{H}$ – $^1\text{H}$  COSY free  $\text{H}_2\text{N}(\text{CH}_2)_5\text{NH}_2$  in  $\text{CDCl}_3$  (Figure S15), DQF-COSY and TOCSY of  $\text{H}_2\text{N}(\text{CH}_2)_5\text{NH}_2$  complexed to bis(ZnII-porphyrin) host (0.3 equiv of guest present in solution) (Figure S16), DQF-COSY free receptor **P(Zn)P(Zn)**, and in the presence of 1.2 equiv of  $\text{H}_2\text{N}(\text{CH}_2)_5\text{NH}_2$  (Figure S17), HYPERQUAD outputs for all UV–vis titrations (Figures S18–S33), Table S1 giving the heat of formation and XYZ coordinates for all the host–guest complexes resulting from theoretical calculations, and Table S2 giving the numerical values of the Soret band shift ( $\Delta\nu$ ) upon complexation with diamines. This material is available free of charge via the Internet at <http://pubs.acs.org>.